

# Identification of Regions of the $\sigma$ -1 Receptor Ligand Binding Site Using a Novel Photoprobe

Arindam Pal, Abdol R. Hajipour, Dominique Fontanilla, Subramaniam Ramachandran, Uyen B. Chu, Timur Mavlyutov, and Arnold E. Ruoho

Department of Pharmacology, University of Wisconsin Medical School, Madison, Wisconsin (A.P., D.F., S.R., U.B.C., T.M., A.E.R.); and Pharmaceutical Research Laboratory, College of Chemistry, Isfahan University of Technology, Isfahan, Iran (A.R.H.)

Received May 18, 2007; accepted July 10, 2007

## ABSTRACT

$\sigma$  Receptors, once considered a class of opioid receptors, are now regarded as a unique class of receptors that contain binding sites for a wide range of ligands, including the drug 1-*N*-(2',6'-dimethylmorpholino)3-(4-*t*-butylpropylamine) (fenpropimorph), a yeast sterol isomerase inhibitor. Because fenpropimorph has high-binding affinity to the  $\sigma$ -1 receptor, we have synthesized a series of fenpropimorph-like derivatives with varying phenyl ring substituents and have characterized their binding affinities to the  $\sigma$ -1 receptor. In addition, we have synthesized a carrier-free, radioiodinated fenpropimorph-like photoaffinity label, 1-*N*-(2',6'-dimethyl-morpholino)-3-(4-azido-3-[<sup>125</sup>I]iodo-phenyl)propane ([<sup>125</sup>I]IAF), which covalently derivatized the  $\sigma$ -1 receptor (25.3 kDa) in both the rat liver and guinea pig liver membranes and the  $\sigma$ -2 receptor (18 kDa) in rat

liver membranes with high specificity. Furthermore, after cleaving the specific [<sup>125</sup>I]IAF-photolabeled  $\sigma$ -1 receptor in guinea pig and rat liver membranes and the pure guinea pig  $\sigma$ -1 receptor with EndoLys-C and cyanogen bromide, the [<sup>125</sup>I]IAF label was identified both in a peptide containing steroid binding domain-like I (SBDLI) (amino acids 91–109) and in a peptide containing steroid binding domain-like II (SBDLII) (amino acids 176–194). Because a single population of binding sites ( $R^2 = 0.992$ ) for [<sup>125</sup>I]IAF interaction with the  $\sigma$ -1 receptor was identified by (+)-[<sup>3</sup>H]pentazocine competitive binding with nonradioactive [<sup>127</sup>I]IAF, it was concluded that SBDLI (amino acids 91–109) and SBDLII (amino acids 176–194) comprises, at least in part, regions of the  $\sigma$ -1 receptor ligand binding site(s).

The  $\sigma$  receptor is a unique receptor that, for the past 30 years, has been persistently enigmatic.  $\sigma$  receptors were initially proposed to be subtypes of opioid receptors based on work performed by Martin and colleagues (1976) to study the actions of antipsychotic drugs. In these experiments, they proposed the existence of a  $\sigma$ -opioid receptor based on the psychomimetic effects of SKF-10047, which could not be explained by  $\mu$ - or  $\kappa$ -opioid receptors (Martin et al., 1976). This hypothesis, however, was later refuted when the  $\sigma$  receptor was shown to be insensitive to naloxone, a common opioid receptor antagonist (Iwamoto, 1981; Su, 1982; Vaupel, 1983). As a result,  $\sigma$  receptors were reclassified as unique nonopioid and nonphencyclidine binding sites present in the central nervous system and peripheral organs that are distinct from

other known neurotransmitter or hormone receptors (Quirion et al., 1992).

To date, two subtypes of the  $\sigma$  receptor have been identified, the  $\sigma$ -1 and  $\sigma$ -2 receptors, which are distinguishable by their pharmacology, function, and molecular mass. The  $\sigma$ -1 receptor was first cloned from guinea pig liver in 1996 (Hanner et al., 1996) and subsequently from other sources, including human placental choriocarcinoma cells (Kekuda et al., 1996), human brain (Prasad et al., 1998), rat brain (Seth et al., 1998; Mei and Pasternak, 2001), and mouse brain (Pan et al., 1998). The  $\sigma$ -2 receptor, however, has yet to be cloned. The  $\sigma$ -1 receptor has 223 amino acids and shares 30% identity and 67% similarity with a yeast sterol C8–C7 isomerase, which is involved in cholesterol synthesis (Moebius et al., 1997). Unlike this yeast sterol isomerase, however, the  $\sigma$ -1 receptor does not have any sterol isomerase activity (Hanner et al., 1996), and it shares no sequence homology with any known mammalian proteins, including the mammalian C8–C7 sterol isomerase.

This work was supported by the National Institutes of Health grant R01-MH065503 (to A.E.R.).

Article, publication date, and citation information can be found at <http://molpharm.aspetjournals.org>.  
doi:10.1124/mol.107.038307.

**ABBREVIATIONS:** SKF-10047, *N*-allyl-normetazocine; IACoc, 3-iodo-4-azido cocaine; IAF, 1-*N*-(2',6'-dimethyl-morpholino)-3-(4-azido-3-iodo-phenyl) propane; SBDLI, sterol binding domain-like I; SBDLII, sterol binding domain-like II; TMD, transmembrane domain; CNBr, cyanogen bromide; PAGE, polyacrylamide gel electrophoresis; DTG, ditolylguanidine; MBP, maltose binding protein; THF, tetrahydrofuran; TLC, thin-layer chromatography; Tricine, *N*-[2-hydroxy-1,1-bis(hydroxymethyl)ethyl]glycine.

In mammalian systems, the  $\sigma$ -1 receptor is ubiquitously expressed in the central nervous system and peripheral organs of the endocrine and immune systems. Because of its broad distribution among tissues, it is speculated that the  $\sigma$ -1 receptor is able to mediate different cellular events such as modulation of voltage-gated  $K^+$  channels (Wilke et al., 1999), calcium release (Hayashi and Su, 2001), regulation of lipid compartmentalization on the endoplasmic reticulum (Hayashi and Su, 2003), regulation of cocaine effects (McCracken et al., 1999a,b), neuroprotective effects (Lysko et al., 1992), increase in extracellular acetylcholine levels (Matsuno et al., 1993), and inhibition of proliferative responses to mitogens (Paul et al., 1994).  $\sigma$ -1 Receptor knockout mice are viable and fertile, showing no overt constitutive phenotype (Langa et al., 2003). Langa and colleagues did find, however, that when the knockout mice were injected with the  $\sigma$  ligand (+)SKF-10047, there was abrogation of the hypermotility response, suggesting a role for  $\sigma$ -1 receptors in psychostimulant actions, which is further supported by the fact that methamphetamine also binds to the  $\sigma$ -1 receptor (Nguyen et al., 2005).

A unique trait of this receptor is that it has high binding affinity for an assorted array of naturally occurring compounds such as steroids and neuropeptides, but it has yet to be determined which, if any, of these compounds are the endogenous ligands for the  $\sigma$ -1 receptor. Pharmacological studies have indicated that this receptor binds to a wide range of compounds including opiates, antipsychotics, antidepressants, antihistamines, phencyclidine-like compounds,  $\beta$ -adrenergic receptor ligands, serotonergic compounds, cocaine and cocaine analogs, neurosteroids, and neuropeptides.

Previous work from our laboratory showed that a cocaine-based radioiodinated photoaffinity label [ $^{125}$ I]3-iodo-4-azido cocaine ([ $^{125}$ I]IACoc) is a high-affinity ligand for the  $\sigma$ -1 receptor (Kahoun and Ruoho, 1992) and specifically identified steroid binding domain-like II (amino acids 176–194) as part of the guinea pig  $\sigma$ -1 receptor binding site for cocaine (Chen et al., 2007). In this article, we report the synthesis and characterization of several fenpropimorph-like ligands that bind to  $\sigma$ -1 and  $\sigma$ -2 receptors as determined in guinea pig liver membranes and rat liver membranes, respectively. The synthesis of the carrier-free, radioiodinated fenpropimorph-like photoaffinity label, 1-*N*-(2',6'-dimethyl-morpholino)-3-(4-azido-3-[ $^{125}$ I]iodo-phenyl)propane ([ $^{125}$ I]IAF), which covalently derivatizes both the  $\sigma$ -1 and  $\sigma$ -2 receptors with high specificity, is reported. In addition,  $\sigma$ -1 receptor binding site peptides that were specifically derivatized by [ $^{125}$ I]IAF upon photolysis have been identified both for the membrane-bound  $\sigma$ -1 receptor and the pure guinea pig  $\sigma$ -1 receptor (Ramachandran et al., 2007) using cleavage strategies with EndoLys-C and cyanogen bromide.

## Materials and Methods

**General.** Melting points were determined with a Thomas-Hoover capillary melting point apparatus and are reported uncorrected. NMR spectra were recorded on a Varian 300 spectrometer with the free-base form of the compounds except where noted (Varian, Palo Alto, CA). Spectra were obtained in  $CDCl_3$  with tetramethylsilane as an internal standard. Chemicals were obtained from Aldrich Chemical Co. (Milwaukee, WI). Elemental analysis was performed by the Research Institute of Petroleum Industry (Tehran, Iran). Frozen rat and guinea pig livers were obtained from Pel-Freez (Rogers, AR).

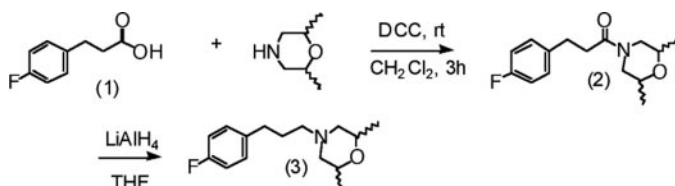
The synthesis of 1-*N*-(2',6'-dimethyl-morpholino)-3-(4-fluoro-3-phenyl propionamide) (**2**) and 1-*N*-(2',6'-dimethyl-morpholino)-3-(4-fluorophenyl-propylamine) (**3**) is outlined in Scheme 1 and that of the remainder of the compounds (**6–11**) is outlined in Scheme 2.

**1-*N*-(2',6'-Dimethyl-morpholino)-3-(4-fluoro-3-phenyl propionamide) (2).** To a solution of dicyclohexylcarbodiimide (**5**) (4.5 g, 22 mmol) in  $CH_2Cl_2$  (120 ml), a mixture of 3-(4-fluoro-3-phenyl) propionic acid (**1**) (3.4 g, 20 mmol) in  $CH_2Cl_2$  (80 ml) was added. After 10 min of stirring at room temperature, 2,6-dimethylmorpholine (22 mmol, 2.5 g) was added drop-wise. The reaction mixture was stirred at room temperature until the starting acid disappeared (3 h) (TLC, hexane/EtOAc, 9:1). The solid was removed by filtration, and the solution was washed with  $H_2O$  ( $2 \times 100$  ml), 10%  $NaHCO_3$  ( $2 \times 100$  ml) before drying with  $MgSO_4$ . The solvent was evaporated by rotary evaporator, and the crude product was purified by column chromatography (silica gel, *n*-hexane/EtOAc, 9:1) as an oil with 90% yield (4.77 g, 18 mmol).  $^1H$  NMR:  $\delta$  7.18 (m, 2 H), 6.97 (m, 2 H), 6.05 (s, 1 H, NH), 3.84 (m, 2 H), 3.43 (d,  $J = 8.1$  Hz, 4H), 2.83 (t, 2 H), 2.51 (t, 2 H), 1.21 (d,  $J = 8.0$  Hz, 6 H).  $^{13}C$ :  $\delta$  173.6, 139.6, 135.0, 129.7 (2 C), 115.9 (2 C), 71.1 (2 C), 57.8 (2 C), 34.5, 31.6, 18.4. Anal. Calcd. for  $C_{15}H_{20}FNO_2$ : C, 67.90; H, 7.55; N, 5.28%. Found: C, 68.00; H, 5.67; N, 6.10%.

**1-*N*-(2',6'-Dimethyl-morpholino)-3-(4-fluorophenyl-propylamine) (3).** In a double-necked round-bottomed flask equipped with septum and condenser, a solution of 1-*N*-(2',6'-dimethyl-morpholino)-3-(4-fluoro-3-phenyl propionamide) (**2**) (2.65 g, 10 mmol) was added drop-wise to a stirred solution of  $LiAlH_4$  (0.74 g, 20 mmol) in anhydrous tetrahydrofuran (THF) (20 ml) under argon. TLC indicated that the reaction was almost completed after 15 min at room temperature. The reaction was driven to completion by brief refluxing (15 min), and the reaction mixture was cooled to room temperature followed by the dilution with 100 ml of THF. The excess  $LiAlH_4$  was destroyed by drop-wise addition of water (3 ml), 15% aqueous NaOH (3 ml), and finally water (10 ml). The reaction mixture was stirred for 30 min at room temperature, and the solids were removed by filtration. The filtrate was dried with  $MgSO_4$  and evaporated by a rotary evaporator to give pure product as yellow oil in 95% yields (2.38 g, 9.5 mmol).  $^1H$  NMR:  $\delta$  7.12 (m, 2 H), 6.95 (m, 2 H), 3.84 (m, 2 H), 3.33 (d,  $J = 8.1$  Hz, 4H), 2.38 (t, 2 H), 2.55 (m, 2 H), 1.72 (t, 2 H), 1.21 (d,  $J = 8.0$  Hz, 6 H).  $^{13}C$ :  $\delta$  160.6, 135.6, 130.0 (2 C), 115.7 (2 C), 71.0 (2 C), 57.8 (2 C), 34.5, 34.6, 32.2 18.6. Anal. Calcd. for  $C_{15}H_{22}FNO$ : C, 71.68; H, 8.82; N, 5.57%. Found: C, 71.59; H, 8.90; N, 5.70%.

**1-*N*-(2',6'-Dimethyl-morpholino)-3-phenyl propane (6).** A mixture of 1-bromo-3-phenyl propane (**4**) (3 mmol, 0.59 g) and 2,6-dimethylmorpholine (**5**) (3.6 mmol, 0.41 g) was refluxed overnight, and the reaction mixture was cooled and purified by column chromatography (silica gel, *n*-hexane/EtOAc, 4:1) in yellow oil in 98% yield (0.6 g, 2.94 mmol).  $^1H$  NMR:  $\delta$  7.21–7.03 (m, 5 H), 3.67 (m, 2 H), 2.65 (m, 4 H), 2.31 (t, 2 H), 1.77 (m, 2 H), 1.69 (t, 2 H), 1.18 (d, 6 H).  $^{13}C$  NMR,  $\delta$  128.46, 126.60, 126.03, 124.12, 73.23, 56.42, 52.25, 39.89, 26.55, 19.31. Anal. Calcd. for  $C_{15}H_{23}NO$ : C, 77.21; H, 9.93; N, 6.00%. Found: C, 77.48; H, 10.03; N, 5.78%.

**1-*N*-(2',6'-Dimethyl-morpholino)-3-(4-nitrophenyl) propane and 1-*N*-(2',6'-dimethyl-morpholino)-3-(2-nitrophenyl) propane (7).** In a round-bottomed flask, a mixture of 1-*N*-(2',6'-dimethyl-morpholino)-3-phenyl propane (**6**) (3 mmol, 0.69 g),  $Bi(NO_3)_3 \cdot 5H_2O$  (1.5 mmol, 0.73 g), and trifluoroacetic anhydride (3 mmol, 0.42 ml) was stirred at room temperature under solvent-free conditions



**Scheme 1.** Schematic diagram for the synthesis of compounds **2** and **3**.

(Hajipour et al., 2003, 2005a,b; Hajipour and Ruoho, 2005a,b). After approximately 5 min, the starting material, 1-*N*-(2',6'-dimethyl-morpholino)-3-phenyl propane (**6**), was consumed (determined by TLC developed in *n*-Hex/EtOAc, 4:1). The product was isolated by precipitation in  $\text{CH}_2\text{Cl}_2$  (20 ml). The solvent was evaporated by a rotary evaporator, and the red residue was purified by column chromatography (silica gel, *n*-hexane/EtOAc, 4:1). The final product (yellow oil) consisted of a mixture of 2- and 4-nitrobenzene isomers in a ratio of 9:1 (the isomers were not separated). The yield of the reaction was 90% (2.7 mmol, 0.75 g).  $^1\text{H}$  NMR:  $\delta$  7.14–8.23 (m, 4 H), 3.67 (m, 2 H), 2.75 (m, 0.4 H), 2.71 (m, 3.6 H), 2.33 (m, 2 H), 1.79 (m, 2 H), 1.69 (m, 2 H), 1.16 (d, 0.6 H), 1.13 (d, 5.4 H).  $^{13}\text{C}$  NMR,  $\delta$  147.25, 144.12, 134.15, 130.25, 128.46, 126.60, 0.126.03, 125.38, 124.12, 73.23, 59.70, 59.40, 58.09, 56.42, 52.25, 39.89, 28.66, 27.78, 26.55, 19.31. Anal. Calcd. for  $\text{C}_{15}\text{H}_{22}\text{N}_2\text{O}_3$ : C, 64.73; H, 7.97; N, 10.06%. Found: C, 64.52; H, 8.13; N, 9.87%.

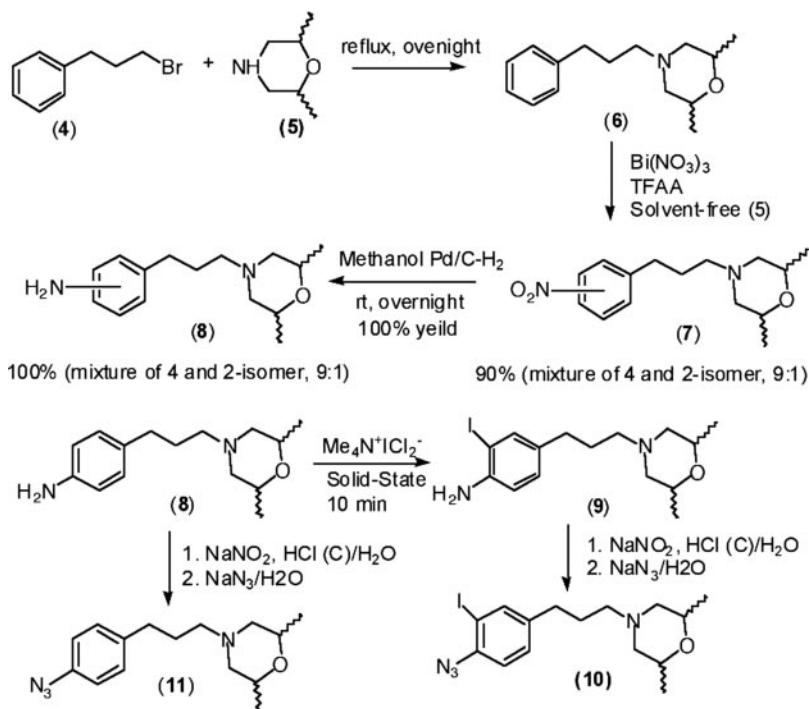
**1-*N*-(2',6'-Dimethyl-morpholino)-3-(4-aminophenyl) propane (8)**. The mixture of 1-*N*-(2',6'-dimethyl-morpholino)-3-(4-nitrobenzene) propane and 1-*N*-(2',6'-dimethyl-morpholino)-3-(2-nitrobenzene) propane (**7**) (3 mmol, 0.83 g) was reduced to the amino derivatives using Pd/C (10%, 0.20 g) in methanol and  $\text{H}_2$  gas overnight. The reaction mixture was filtered to give 1-*N*-(2',6'-dimethyl-morpholino)-3-(aminophenyl) propane (**8**) as a mixture of 2- and 4-aminobenzene isomers in 96% yield (2.88 mmol, 0.71 g). The 1-*N*-(2',6'-dimethyl-morpholino)-3-(4-aminobenzene) propane isomer was separated from 1-*N*-(2',6'-dimethyl-morpholino)-3-(2-aminobenzene) propane by column chromatography (silica gel, *n*-hexane/EtOAc, 4:1) (90%, 0.64 g). Yellow oil.  $^1\text{H}$  NMR:  $\delta$  7.13 (d,  $J = 8.4$ , 2 H), 6.63 (d,  $J = 8.4$ , 2 H), 4.80 (br, 2 H,  $\text{NH}_2$ ), 3.75 (m, 2 H), 2.74 (m, 4 H), 2.62 (t, 2 H), 2.22 (m, 2 H), 1.85 (t, 2 H), 1.18 (d, 6 H).  $^{13}\text{C}$  NMR,  $\delta$  129.93, 126.24, 118.46, 115.24, 71.73, 59.69, 58.43, 32.84, 26.46, 19.30. Anal. Calcd. for  $\text{C}_{15}\text{H}_{24}\text{N}_2\text{O}$ : C, 72.54; H, 9.74; N, 12.28%. Found: C, 72.68; H, 9.86; N, 12.68%.

**1-*N*-(2',6'-Dimethyl-morpholino)-3-(4-amino-3-iodo-phenyl) propane (9)**. In a mortar, a mixture of 1-*N*-(2',6'-dimethyl-morpholino)-3-(4-aminophenyl) propane (**8**) (3 mmol, 0.74 g),  $\text{Me}_4\text{N}^+\text{ICl}_2^-$  (3.6 mmol, 1.0 g) was ground with a pestle under solid-state conditions for 30 min to afford 1-*N*-(2',6'-dimethyl-morpholino)-3-(4-amino-3-iodo-phenyl) propane (**9**). The reaction mixture was dissolved in a mixture of water and ethyl acetate (100 ml, 1:1). The organic layer

was separated, and the aqueous layer was extracted with ethyl acetate ( $2 \times 25$  ml). The combined ethyl acetate solution was dried ( $\text{MgSO}_4$ ), decolorized with activated charcoal (2 g), and filtrated. The solvent was evaporated with a rotary evaporator to afford 1-*N*-(2',6'-dimethyl-morpholino)-3-(4-amino-3-iodo-phenyl) propane (**9**) as a yellowish oil, 90% yield (2.7 mmol, 1.01 g). The crude product was used for the next step without purification.

**1-*N*-(2',6'-Dimethyl-morpholino)-3-(4-azido-3-iodo-phenyl) propane (10)**. In a round-bottomed flask, 1-*N*-(2',6'-dimethyl-morpholino)-3-(4-amino-3-iodo-phenyl) propane (**9**) (3 mmol, 1.12 g) was dissolved in 20% HCl (v/v) and allowed to stand for 5 min at  $0^\circ\text{C}$ .  $\text{NaNO}_2$  (3.6 mmol, 0.21 g, in 5 ml of  $\text{H}_2\text{O}$ ) was then added, and the reaction mixture was stirred at room temperature for 30 min. An aqueous solution of  $\text{NaN}_3$  (3.6 mmol, 0.23 g, in 5 ml of  $\text{H}_2\text{O}$ ) was added drop-wise to the reaction mixture. The reaction was stirred at room temperature in the dark for 30 min and then extracted with ethyl acetate ( $3 \times 30$  ml). The combined ethyl acetate extracts were dried with  $\text{MgSO}_4$ , and the solvent was evaporated using a rotary evaporator to afford an orange oil. The crude product was purified by column chromatography (silica gel, initially toluene/ $\text{Et}_2\text{NH}$ , 20:1, followed by toluene/ $\text{Et}_2\text{NH}$ , 4:1). Yield, 95%, (2.85 mmol, 1.14 g), Yellowish oil.  $^1\text{H}$  NMR:  $\delta$  8.40 (d,  $J = 1.8$ , 1 H), 8.20 (dd,  $J = 1.8$ , 8.4 1 H), 7.2 (d,  $J = 8.4$ , 1 H), 3.75 (m, 2 H), 2.74 (m, 4 H), 2.62 (t, 2 H), 2.22 (m, 2 H), 1.85 (t, 2 H), 1.18 (d, 6 H).  $^{13}\text{C}$  NMR,  $\delta$  158.90, 139.10, 135.25, 130.20, 128.10, 127.40, 71.61, 59.73, 58.43, 32.84, 26.46, 19.30. Anal. Calcd. for  $\text{C}_{15}\text{H}_{22}\text{IN}_4\text{O}$ : C, 44.90; H, 5.53; N, 13.96%. Found: C, 45.11; H, 5.79; N, 13.74%.

**1-*N*-(2',6'-Dimethyl-morpholino)-3-(4-azidophenyl) propane (11)**. This reaction was performed as described above using 1-*N*-(2',6'-dimethyl-morpholino)-3-(4-aminophenyl) propane (**8**) (3 mmol, 0.74 g) as the starting material. The crude product was purified by column chromatography as described above (silica gel, first toluene/ $\text{Et}_2\text{NH}$ , 20:1, and then toluene/ $\text{Et}_2\text{NH}$ , 4:1) to yield 1-*N*-(2',6'-dimethyl-morpholino)-3-(4-azidophenyl) propane (**11**) in 96% yield (0.26 g, 2.88 mmol), m.p. 128–131.  $^1\text{H}$  NMR,  $\delta$  7.92 (d,  $J = 8.4$ , 2 H), 7.23 (d,  $J = 8.4$ , 2 H), 3.72 (m, 2 H), 2.74 (m, 4 H), 2.62 (t, 2 H), 2.22 (m, 2 H), 1.85 (t, 2 H), 1.18 (d, 6 H).  $^{13}\text{C}$  NMR,  $\delta$  142.13, 135.25, 130.20, 128.40, 71.61, 59.73, 58.43, 32.84, 26.46, 19.30. Anal. Calcd. for  $\text{C}_{15}\text{H}_{23}\text{N}_4\text{O}$ : C, 65.43; H, 8.42; N, 20.35%. Found: C, 64.29; H, 8.59; N, 20.54%.



**Scheme 2.** Schematic diagram for the synthesis of compounds **6**, **7**, **8**, **9**, **10**, and **11**.

**Radio-synthesis of [<sup>125</sup>I]IAF.** Radioactive Na[<sup>125</sup>I] (5 mCi) in 14 μl of 0.1 M NaOH was neutralized by adding 14 μl of 0.1 M HCl and then diluted with 50 μl of 0.5 M sodium acetate buffer, pH 5.6. 1-*N*-(2',6'-dimethyl-morpholino)-3-(4-amino-phenyl) propane (10 μl of 2.5 mg/ml in 0.5 M sodium acetate buffer, pH 5.6) was then added to the reaction. Iodination was initiated by adding 30 μl of Chloramine-T (1 mg/ml in water) and continued for 15 min at room temperature. The reaction was terminated by the addition of 100 μl of Na<sub>2</sub>S<sub>2</sub>O<sub>5</sub> (5 mg/ml in water). The pH of the reaction was adjusted to approximately 9 by adding 20 μl of 1 M NaOH. The reaction mixture was then extracted three times with 1 ml of ethyl acetate. The pooled extracts were evaporated under N<sub>2</sub> to approximately 50 μl and streaked on a 0.25-mm thick silica gel (60/254) plate (10 × 20 cm), which was developed with a solvent system of toluene/diethylamine (4:1 v/v). 1-*N*-(2',6'-Dimethyl-morpholino)-3-(4-amino-3-[<sup>125</sup>I]iodo-phenyl)propane was detected by autoradiography using X-Omat film (*R<sub>f</sub>* = 0.63) (Eastman Kodak, Rochester, NY), and the corresponding silica gel was extracted three times with 1 ml of ethyl acetate and stored at -20°C (yield, 1.5 mCi, 30%).

The ethyl acetate extract of 1-*N*-(2',6'-imethyl-morpholino)-3-(4-amino-3-[<sup>125</sup>I]iodo-phenyl)propane was evaporated to dryness under an N<sub>2</sub> stream. H<sub>2</sub>SO<sub>4</sub> (50 μl of 3%) was added to the tube, vortexed, and kept on ice for approximately 15 min. To this reaction mixture, 10 μl of 1 M sodium nitrite was added and maintained on ice in the dark for 30 min. Sodium azide (50 μl of 1 M) was added, and the reaction was allowed to proceed on ice in the dark for 30 min. The reaction was terminated by the addition of 0.5 ml of 10% sodium bicarbonate and then extracted three times with 1 ml of ethyl acetate. The extracts were pooled and back-extracted with 0.5 ml of water. The extract was then reduced to approximately 50 μl under an N<sub>2</sub> stream and streaked on a 0.25-mm thick silica gel (60/254) plate (10 × 20 cm), which was developed in toluene/diethylamine (20:1). The major radioactive reaction product, [<sup>125</sup>I]IAF, migrated with an *R<sub>f</sub>* value of 0.81. The material was detected by autoradiography, and the corresponding silica gel was extracted three times with ethyl acetate and stored at -20°C overnight. The ethyl acetate extract was centrifuged the next day at 24,000 rpm for 10 min to remove dissolved silica (appeared as a solid white precipitate). The radioactive product comigrated with authentic nonradioactive 1-*N*-(2',6'-imethyl-morpholino)-3-(4-azido-3-iodo-phenyl) propane prepared as described above. The overall yield for the synthesis of [<sup>125</sup>I]IAF varied between 18 and 20%.

**Preparation of Rat Liver and Guinea Pig Liver Membranes.** Minced frozen rat livers or guinea pig livers (65 g) were thawed in 100 ml of homogenization buffer (10 mM phosphate buffer, pH 7.4, containing 0.32 M sucrose, 1 M MgSO<sub>4</sub>, 0.5 M EGTA, 1 mM phenyl-methylsulfonyl fluoride, 10 μg/ml leupeptin, 1 μg/ml pepstatin A, and 10 μg/ml *p*-toluenesulfonyl-L-arginine methyl ester) and then homogenized on ice with a homogenizer (setting 6, four bursts of 10-s each; Polytron; Kinematica, Basel, Switzerland) followed by a glass homogenizer (Teflon pestle by six slow passes at 3000 rpm). The homogenized tissues were then centrifuged at 17,000g for 10 min. The supernatants were re-centrifuged at 100,000g for 1 h. The microsomal pellets were resuspended in homogenization buffer, snap-frozen with dry ice/ethanol, and stored at -80°C at a final protein concentration of 20 mg/ml.

**Preparation of Pure Guinea Pig σ-1 Receptor.** Pure guinea pig σ-1 receptor was prepared as reported previously (Ramachandran et al., 2007). In brief, the maltose binding protein (MBP)-guinea pig σ-1 receptor fusion protein with a Factor Xa cleavage site linking the MBP and σ-1 receptor and a six-histidine tag on the C terminus of σ-1 receptor was expressed in *Escherichia coli*. The *E. coli* biomass was collected by centrifugation at 3000 rpm for 30 min, sonicated for 15 min at 4°C, centrifuged at 100,000g for 1 h at 4°C and the pellet resuspended, and extracted for 3 h with stirring at 4°C in 20 mM Tris, pH 8.0, 0.2 M NaCl, 1 mM 2-mercaptoethanol, and 1 mM EDTA supplemented with a protease inhibitor cocktail and Triton X-100. The extract was centrifuged at 100,000g for 1 h at 4°C. The supernatant containing the

fusion protein was then purified on an amylose column and cleaved with Factor Xa at room temperature for 36 to 48 h. The σ-1 receptor with a six-histidine tag at the C terminus was collected on an Ni<sup>2+</sup> column and eluted using 0.25 M imidazole in wash buffer (50 mM sodium phosphate, pH 8.0, and 0.3 M NaCl) containing 1% Triton X-100. The protein that was eluted from the Ni<sup>2+</sup> column was further purified by incubating with an agarose resin coupled with anti-Maltose binding protein antibody (binding capacity of approximately 0.4 mg for MBP per milliliter) at 4°C for 18 to 24 h. After incubation was complete, the mixture was centrifuged at 4000 rpm at room temperature, and the supernatant contained pure guinea pig σ-1 receptor containing a six-histidine tag at the C terminus.

**σ Receptor Binding Assays.** The binding affinities of the newly synthesized compounds for the σ-1 and σ-2 receptors were determined using competitive binding assays as described previously (Matsumoto et al., 1995; Nguyen et al., 2005). Assays for σ-1 receptors were performed using (+)-[<sup>3</sup>H]pentazocine (10 nM) in guinea pig liver membranes (25 μg/well) incubated at 30°C for 1 h with several

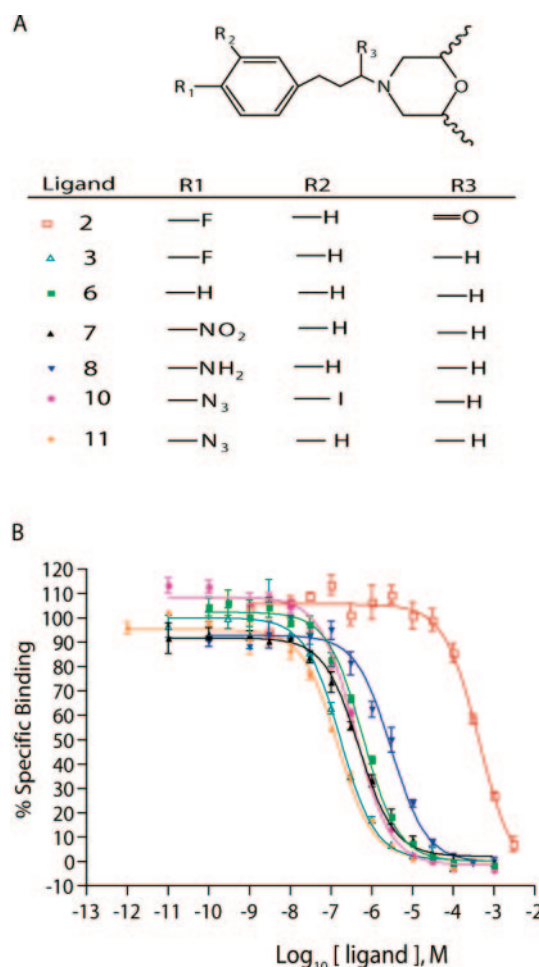


**Fig. 1.** A, structures of the different fenpropimorph derivatives used in competitive binding assays. B, inhibition of (+)-[<sup>3</sup>H]pentazocine binding by fenpropimorph derivatives in guinea pig liver membranes. Competitive binding curves against 10 nM (+)-[<sup>3</sup>H]pentazocine were generated for the fenpropimorph derivatives, and data points were fit to a one-site nonlinear regression curve. Haloperidol (5 μM) was used to determine nonspecific binding. The *K<sub>D</sub>* values for compounds were calculated using GraphPad Prism software (version 4.0c) and are listed in Table 1. Compound 2 was found not to bind to the σ-1 receptor (*K<sub>D</sub>* > 100 μM). Compounds 3 and 11 had *K<sub>D</sub>* values of 84 ± 21.9 and 72.3 ± 14.9 nM, respectively. Compounds 6, 7, and 8 had low affinities for σ-1 receptor and had *K<sub>D</sub>* values of 301 ± 61.7, 242 ± 47, and 1500 ± 390 nM, respectively. IAF (compound 10) had moderate affinity to the σ-1 receptor with a *K<sub>D</sub>* value of 194 ± 27.5 nM.

concentrations of competing ligands showed in Fig. 1A. After incubation, the guinea pig liver membranes were harvested on a 0.5% polyethylenimine-treated Whatman GF/B filters using a Brandel cell harvester (Brandel, Gaithersburg, MD). The assay for determining the  $\sigma$ -2 binding property of IAF was performed using rat liver membranes (25  $\mu$ g/well) and 30 nM [ $^3$ H]ditolylguanidine (DTG) in the presence of (+)-pentazocine (100 nM). Haloperidol (5  $\mu$ M) was used to determine nonspecific binding for both  $\sigma$ -1 and  $\sigma$ -2 receptor binding assays. Radioactivity on the filters was detected by liquid scintillation spectrometry using NEN formula 989 as scintillation cocktail (PerkinElmer Life and Analytical Sciences, Waltham, MA). The values were fit to a nonlinear regression curve using the software GraphPad Prism version 4.0c (GraphPad Software Inc., San Diego, CA), and reported dissociation equilibrium constants,  $K_D$ , were calculated using the Cheng-Prusoff equation (Cheng and Prusoff, 1973).

**Photoaffinity Labeling of the Rat and Guinea Pig Liver Membrane  $\sigma$ -1 Receptor.** Rat or guinea pig liver membranes (200  $\mu$ g/tube) were suspended in a final volume of 0.1 ml of incubation buffer (50 mM Tris-HCl, pH 7.4) in the presence or absence of the protecting drugs and incubated at 37°C for 20 min. [ $^{125}$ I]IACoc (Kahoun and Ruoho, 1992; Chen et al., 2007) or [ $^{125}$ I]IAF was added to the membrane suspensions to a final concentration of 1 nM (1% ethyl acetate, final concentration) and again incubated for 15 min at 37°C. The tubes containing membrane suspensions were then placed in an ice-cold water bath in the photoreactor, and the membrane suspensions were diluted 10-fold with ice-cold incubation buffer containing 20 mM  $\beta$ -mercaptoethanol immediately before photolysis. Activation of the photoaffinity labels was accomplished by exposure to a high-pressure AH-6 mercury lamp (Advanced Radiation Corporation, Santa Clara, CA) from a distance of 10 cm for 6 s. After photolysis, membrane suspensions were centrifuged at 100,000g for 1 h at 4°C, and the pellets were resuspended in 0.1 ml of incubation buffer. Proteins were separated by 16.5% SDS-tricine/PAGE and visualized by PhosphorImager (GE Healthcare, Chalfont St. Giles, Buckinghamshire, UK).

**Photoaffinity Labeling of the Pure Guinea Pig  $\sigma$ -1 Receptor.** The pure guinea pig  $\sigma$ -1 receptor (10  $\mu$ g/tube) in 100  $\mu$ l of incubation buffer containing 20 mM  $\beta$ -mercaptoethanol was incubated at 37°C for 20 min in the presence or absence of the protecting  $\sigma$ -1 ligands. [ $^{125}$ I]IACoc or [ $^{125}$ I]IAF was then added to each tube to a final concentration of 1 nM (1% ethyl acetate, final concentration) and again incubated for 15 min at 37°C as described above. The tubes were then placed in the ice-cold water bath of the photoreactor and photolysed as described above for 6 s. After photolysis, 5 $\times$  SDS-PAGE sample buffer (25  $\mu$ l/tube) was added before separation by 16.5% SDS-Tricine/PAGE and finally visualized by PhosphorImaging.

**EndoLys C Digestion of the Photolabeled  $\sigma$ -1 Receptor.** Before the enzymatic cleavage with the EndoLys C, the  $\sigma$ -1 receptor was photolabeled separately (10  $\mu$ g of pure protein in 100  $\mu$ l of incubation buffer per tube or 1 mg of rat and guinea pig liver membrane separately in 1 ml of incubation buffer per tube) in the presence and absence of the protector (10  $\mu$ M haloperidol) using both [ $^{125}$ I]IACoc (1 nM) and [ $^{125}$ I]IAF (1 nM) as described above. Photolabeled samples were purified by electrophoresis on a 15% SDS-polyacrylamide gel and visualized by wet gel (unstained) autoradiography. The autoradiogram was used as a template to excise the specifically labeled and the protected  $\sigma$ -1 receptor from the gel with a razor blade. The gel slices were minced and placed into a 1.5-ml microcentrifuge tube containing 1 ml of water. The tubes were maintained overnight at 4°C, and the gel slurries were transferred to spin columns (Bio-Rad Laboratories, Hercules, CA). The eluted  $\sigma$ -1 receptor in the supernatant extract was collected by centrifugation at 1600g for 5 min. In general, more than 80% of the photolabeled  $\sigma$ -1 receptor was recovered in the aqueous supernatant (as measured by radioactivity). The eluted materials were concentrated to 100  $\mu$ l by lyophilization and incubated with 0.25  $\mu$ g of EndoLys C (Promega, Madison, WI) per tube overnight at room temperature. The enzymatic digestions were terminated by adding 5 $\times$  SDS-PAGE sample

buffer and separated by 16.5% SDS-Tricine/PAGE. The peptides were again identified by wet-gel autoradiography, excised, and eluted with water as described above. The eluted peptides were concentrated (to approximately 30  $\mu$ l) and subjected to cyanogen bromide (CNBr) digestion separately.

**CNBr Digestion of the  $\sigma$ -1 Receptor Peptides.** The concentrated peptides were mixed with 70  $\mu$ l of CNBr solution (0.15 M in 70% formic acid solution) for 15 to 18 h at room temperature by tumbling. The reaction mixtures were then diluted with 1 ml of water, lyophilized, and separated by 16.5% SDS-Tricine/PAGE. Gels were stained-destained, dried, and the radiolabeled peptides were visualized by PhosphorImaging.

## Results

**Chemistry.** The synthesis of fenpropimorph derivatives **2** and **3** is outlined in Scheme 1. 1-*N*-(2',6'-dimethyl-morpholino)-3-(4-fluoro-3-phenyl propionamide) (**2**) was obtained by activating the carbonyl group of 3-(4-fluoro-3-phenyl) propionic acid (starting material is designated as compound **1**) with dicyclohexylcarbodiimide followed by stirring at room temperature with 2,6-dimethyl morpholine. The crude product was purified by silica gel column chromatography using *n*-hexane and ethyl acetate mixture at a ratio of 9:1 as the solvent system. 1-*N*-(2',6'-dimethyl-morpholino)-3-(4-fluorophenyl-propylamine) (**3**) was obtained by reduction of (**2**) with lithium aluminum hydride (LiAlH<sub>4</sub>) in anhydrous THF under argon. After 15-min incubation at room temperature and a 15-min reflux, the LiAlH<sub>4</sub> was destroyed by aqueous base at room temperature, and solids were removed by filtration. The filtrate yielded pure product as a yellow oil.

The synthesis of fenpropimorph derivatives **4** to **11** is outlined in Scheme 2. 1-*N*-(2',6'-dimethyl-morpholino)-3-phenyl propane (**6**) was obtained by refluxing a mixture of 1-bromo-3-phenyl propane (**4**) and 2,6-dimethylmorpholine (**5**) overnight, and the reaction mixture was purified by column chromatography (silica gel, *n*-hexane/EtOAc, 4:1) as a yellow oil in 98% yield. The 1-*N*-(2',6'-dimethyl-morpholino)-3-phenyl propane (**6**) was reacted with Bi(NO<sub>3</sub>)<sub>3</sub> in trifluoroacetic anhydride under solvent-free conditions to afford a mixture of 1-*N*-(2',6'-dimethyl-morpholino)-3-(4-nitrophenyl) propane and 1-*N*-(2',6'-dimethyl-morpholino)-3-(2-nitrophenyl) propane (**7**) in a ratio of 90:10 in 100% yield (<sup>1</sup>H NMR analysis). The mixture of 1-*N*-(2',6'-dimethyl-morpholino)-3-(4-nitrophenyl) propane and 1-*N*-(2',6'-dimethyl-morpholino)-3-(2-nitrophenyl) propane (**7**) was reduced to 1-*N*-(2',6'-dimethyl-morpholino)-3-(4-aminophenyl)propane and 1-*N*-(2',6'-dimethyl-morpholino)-3-(2-aminophenyl)propane (**8**) in methanol with Pd/C-H<sub>2</sub> in 96% yield. The 1-*N*-(2',6'-dimethyl-morpholino)-3-(4-aminophenyl)propane was separated from 1-*N*-(2',6'-dimethyl-morpholino)-3-(2-aminophenyl)propane by column chromatography (silica gel, *n*-hexane/EtOAc, 4:1). Reaction of 1-*N*-(2',6'-dimethyl-morpholino)-3-(4-aminophenyl) propane (**8**) with Me<sub>4</sub>N<sup>+</sup>ICl<sub>2</sub><sup>-</sup> under solid-state conditions afforded 1-*N*-(2',6'-dimethyl-morpholino)-3-(4-amino-3-iodo-phenyl) propane (**9**) as a yellowish oil. The crude 1-*N*-(2',6'-dimethyl-morpholino)-3-(4-amino-3-iodophenyl) propane (**9**) was reacted with HNO<sub>2</sub> and then NaN<sub>3</sub> to produce 1-*N*-(2',6'-dimethyl-morpholino)-3-(4-azido-3-iodophenyl) propane (**10**) in excellent yields after purification. The 1-*N*-(2',6'-dimethyl-morpholino)-3-(4-azidophenyl) propane (**11**) was also prepared by reacting 1-*N*-(2',6'-dime-

thyl-morpholino)-3-(4-aminophenyl) propane (**8**) with  $\text{HNO}_2$  and then with  $\text{NaN}_3$  in excellent yield.

**Binding of Fenpropimorph Derivatives to  $\sigma$ -1 and  $\sigma$ -2 Receptors.** All fenpropimorph derivatives (structures shown in Fig. 1A) were tested for binding affinities to  $\sigma$ -1 receptors in guinea pig liver membranes, and IAF (compound **10**) binding to the  $\sigma$ -2 receptor was determined in rat liver membranes. The binding affinities of these compounds were determined by competition of (+)-[ $^3\text{H}$ ]pentazocine (10 nM) with high affinity and selectivity to the  $\sigma$ -1 receptor. For IAF binding to the  $\sigma$ -2 receptor, 30 nM [ $^3\text{H}$ ]DTG was used in the presence of nonradioactive (+)-pentazocine (100 nM).

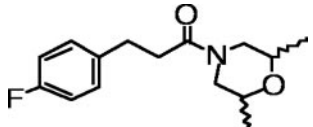
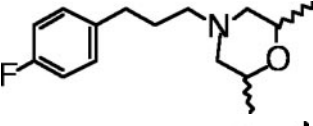
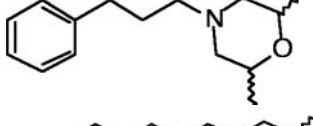
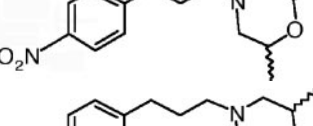
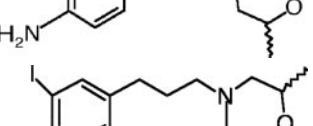
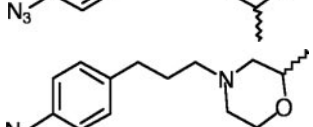
The curves obtained for the  $\sigma$ -1 receptor competition assays are shown in Fig. 1B, and the results are summarized in Table 1. Two of the seven compounds presented (**3** and **11**) had high affinities for the  $\sigma$ -1 receptor with  $K_D$  values of less than 100 nM. The iodo-azido derivative or IAF (compound **10**) had  $K_D$  values of  $194 \pm 27.5$  nM and  $2.78 \pm 1.5$   $\mu\text{M}$  for the  $\sigma$ -1 and the  $\sigma$ -2 receptor, respectively. Linear regression curve fitting indicated that all the compounds, including IAF, fit to a single population of binding sites for the  $\sigma$ -1 receptor with  $R^2$  values between 0.951 and 0.992 (Table 1).

**Photoaffinity Labeling of  $\sigma$  Receptors in Rat Liver Microsomal Membranes.** Both [ $^{125}\text{I}$ ]IACoc and [ $^{125}\text{I}$ ]IAF

were used to covalently derivatize the  $\sigma$  receptors from rat microsomes (Fig. 2A), and specific labeling of both the  $\sigma$ -1 and  $\sigma$ -2 receptors was observed. The  $\sigma$ -1 receptor was shown to be a 25.3-kDa band, which was protected by nonradioactive (+)-pentazocine (100 nM), haloperidol (10  $\mu\text{M}$ ), DTG (25  $\mu\text{M}$ ), and fenpropimorph (10  $\mu\text{M}$ ), whereas the  $\sigma$ -2 receptor photolabeling at 18 kDa was protected by haloperidol, DTG, and fenpropimorph but not by the  $\sigma$ -1-selective ligand, pentazocine (Fig. 2B). Compared with the robust  $\sigma$ -1-specific labeling of the cocaine-based radioiodinated photoaffinity label, [ $^{125}\text{I}$ ]IACoc, the fenpropimorph-like photoprobe [ $^{125}\text{I}$ ]IAF specifically derivatized both the  $\sigma$ -1 and  $\sigma$ -2 receptors (Fig. 2A). Several additional specifically photolabeled bands are also detected at 96.7, 130, and 147.3 kDa, as assessed from a plot of  $R_f$  versus log molecular mass of the standards (Fig. 2A, inset). The high molecular mass bands present appeared after photolysis with both [ $^{125}\text{I}$ ]IACoc and [ $^{125}\text{I}$ ]IAF (Fig. 2A) and were each protected by (+)-pentazocine, haloperidol, DTG, and fenpropimorph (Fig. 2B). A band at 19 kDa was also highly specifically labeled with [ $^{125}\text{I}$ ]IAF (Fig. 2, A and B). Photolabeling of this 19-kDa band was not protected by (+)-pentazocine or haloperidol but was partially protected by DTG (Fig. 2B) and completely protected by nonradiolabeled fenpropimorph.

TABLE 1

$\sigma$ -1 Receptor affinity ( $K_D$ ) and one-site linear regression analysis of fenpropimorph derivatives as determined in guinea pig liver membranes.  $K_D$  and  $R^2$  values of these compounds were calculated using GraphPad Prism software, version 4.0c.

Ligands	Structures	$\sigma$ -1 $K_D \pm$ S.E.M. <sup>a</sup>	$R^2$ Value (One-Site Linear Regression)
		<i>nM</i>	
<b>2</b>		>200,000	0.951
<b>3</b>		$84 \pm 21.9$	0.978
<b>6</b>		$301 \pm 61.7$	0.986
<b>7</b>		$242 \pm 47.0$	0.988
<b>8</b>		$1500 \pm 390$	0.978
<b>10</b>		$194 \pm 27.5$	0.992
<b>11</b>		$72.3 \pm 14.9$	0.986

<sup>a</sup> Mean of triplicate experiments  $\pm$  S.E.M.

**Photoaffinity Labeling of  $\sigma$  Receptors in Guinea Pig Liver Microsomal Membranes.** Both [ $^{125}$ I]IACoc and [ $^{125}$ I]IAF specifically and covalently derivatized the  $\sigma$ -1 receptor from guinea pig liver membranes (Fig. 3A, right). Using both probes, the  $\sigma$ -1 receptor was detected as a 25.3-kDa band, which was protected by haloperidol (10  $\mu$ M). Compared with the rat liver membranes (Fig. 3A, left), the  $\sigma$ -2 receptors and the high molecular mass bands were not observed with either photoprobe in the guinea pig liver membranes.

**EndoLys C Digestion of [ $^{125}$ I]IACoc and [ $^{125}$ I]IAF Specifically Photolabeled  $\sigma$ -1 Receptor in Rat and Guinea Pig Liver Microsomal Membranes.** Figure 3A demonstrates labeling of the rat liver and guinea pig liver membranes with [ $^{125}$ I]IACoc and [ $^{125}$ I]IAF. The labeling of the  $\sigma$ -1 receptor in both membrane preparations was highly specific (compare lanes 1, 3, 5, and 7 with 2, 4, 6, and 8, respectively, in Fig. 3A) in the presence and absence of 10  $\mu$ M

haloperidol. The 25.3-kDa band, which showed specific labeling by both photoprobes, was excised (region outlined by the broken lines) and eluted with water. Generally, 80% of the [ $^{125}$ I]iodine-photolabeled  $\sigma$ -1 receptor was eluted.

Before EndoLys C cleavage, the starting specifically photolabeled  $\sigma$ -1 receptors, as eluted from the gels, are shown in the autoradiogram in Fig. 3C (lanes 1 and 2, 5 and 6, 9 and 10, and 13 and 14). EndoLys-C cleavage, as depicted in the cleavage at lysine 142 in Fig. 3B, resulted the eluted [ $^{125}$ I]iodine photolabeled  $\sigma$ -1 receptor into two large fragments of 16.3 and 9 kDa (Fig. 3C, lanes 3, 7, 11, and 15). Specificity of the photoprobe (i.e., haloperidol protection) and subsequent cleavage is further shown in Fig. 3C (lanes 4, 8, 12, and 16). No EndoLys-C cleavage was observed at lysine 60 in the guinea pig  $\sigma$ -1 receptor.

As reported previously (Chen et al., 2007), [ $^{125}$ I]IACoc specifically labeled the SBDLII domain (amino acids 170–195) at Asp188, which corresponds to the 9-kDa fragment (Fig. 3C,

A

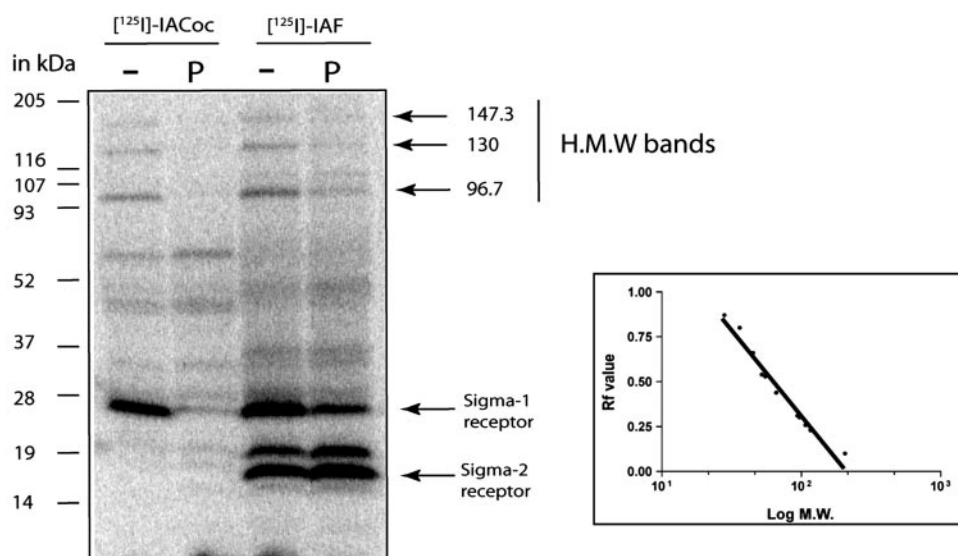
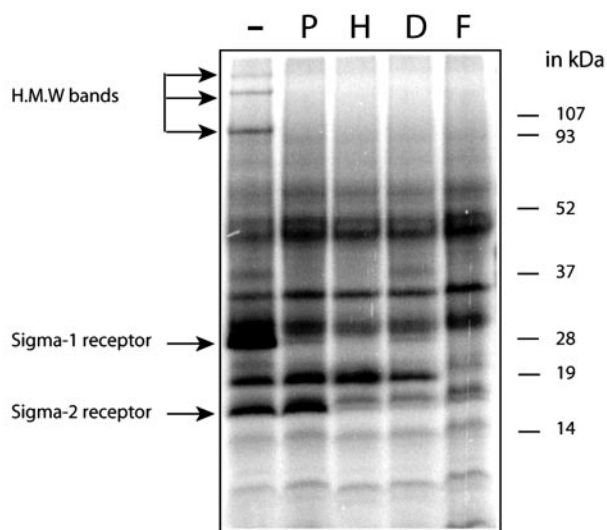


**Fig. 2.** A, comparison of photolabeling the  $\sigma$ -1 and  $\sigma$ -2 receptor using [ $^{125}$ I]IACoc and [ $^{125}$ I]IAF. Rat liver microsomes (200  $\mu$ g/lane) were photolabeled using 1 nM [ $^{125}$ I]IACoc and [ $^{125}$ I]IAF separately with no protector (-) and in the presence of 100 nM (+)pentazocine (P). Both photoprobes labeled the  $\sigma$ -1 receptor and three high molecular mass (+)pentazocine-protectable protein bands. The molecular masses of these three bands were calculated from the standard curve obtained by plotting  $R_f$  values against the Log(molecular mass) of various known protein standards, which ranged between 205 and 14 kDa (inset). B, [ $^{125}$ I]IAF labeling of rat liver microsomes. Photolabeling of rat liver microsomes (200  $\mu$ g/lane) with 1 nM [ $^{125}$ I]IAF with no protector (-) and in the presence of 100 nM (+)pentazocine (P), 10  $\mu$ M haloperidol (H), 25  $\mu$ M DTG (D), and 10  $\mu$ M fenpropimorph (F). Photolabeling was performed as described under *Materials and Methods*, and the proteins were separated by SDS-Tricine/PAGE.

B





cleavage of the pure guinea pig  $\sigma$ -1 receptor (Fig. 4B) was also observed after photolabeling by [ $^{125}$ I]IACoc and [ $^{125}$ I]IAF, as shown previously in Fig. 3C for the guinea pig liver membrane  $\sigma$ -1 receptor. In these experiments, the pure  $\sigma$ -1 receptor (Fig. 4B, lanes 1 and 2) was cleaved by EndoLys-C and produced the same two polypeptides (Fig. 4B, lanes 3 and 4), as assessed by Coomassie staining, but the peptide containing SBDLII now migrated at 9.8 kDa instead of the 9-kDa position (from the membrane-bound receptor) because the pure guinea pig  $\sigma$ -1 receptor contains six histidine residues at the C terminus. Specific photolabeling by [ $^{125}$ I]IACoc and [ $^{125}$ I]IAF, as illustrated in the autoradiogram in Fig. 4B, lanes 5 and 6 and lanes 10 and 11, again showed that the cleavage of the photolabeled receptor with EndoLys-C produced the expected [ $^{125}$ I]IACoc-labeled 9.8-kDa peptide containing SBDLII (Fig. 4B, lanes 7 and 8). On the other hand, EndoLys-C cleavage of the [ $^{125}$ I]IAF photolabeled receptor showed labeling of both the 16.3- and the 9.8-kDa peptides (Fig. 4B, lanes 12 and 13) indicating, as was the case for the membrane-bound receptor (Fig. 3C), that [ $^{125}$ I]IAF labeled the  $\sigma$ -1 receptor binding site at two posi-

tions, consistent with the SBDLI- and SBDLII-containing peptides. There may be weak cleavage at lysine 60 in the pure receptor, as indicated in Fig. 4C (lane 12) at 9.3 kDa, because cleavage at position 60 would produce a peptide from residues 60 to 142, which also contains the SBDLI (91–109) region.

**CNBr Cleavage of the 16.3- and 9.8-kDa Peptides Derived from EndoLys-C Cleavage of the Photolabeled Pure Guinea Pig  $\sigma$ -1 Receptor.** Before cleavage by cyanogen bromide, the 16.3- and 9.8-kDa peptides, as shown with Coomassie staining (Fig. 5B, lanes 1–4), was eluted from SDS gels. For both [ $^{125}$ I]IACoc and [ $^{125}$ I]IAF-labeled peptides, the Coomassie staining patterns were identical, and therefore, only the staining pattern for the [ $^{125}$ I]IACoc-labeled peptides is shown for both EndoLys-C cleavage (Fig. 5B) and subsequent CNBr cleavage (Fig. 5C). Because the CNBr cleavage experiments required more peptide material, the photolabeling intensity as shown in Fig. 5B (lanes 5–12) was more intense than observed in Fig. 4B but produced qualitatively and quantitatively the same relative results. Specific photolabeling of [ $^{125}$ I]IACoc was protected only at the 9.8-kDa

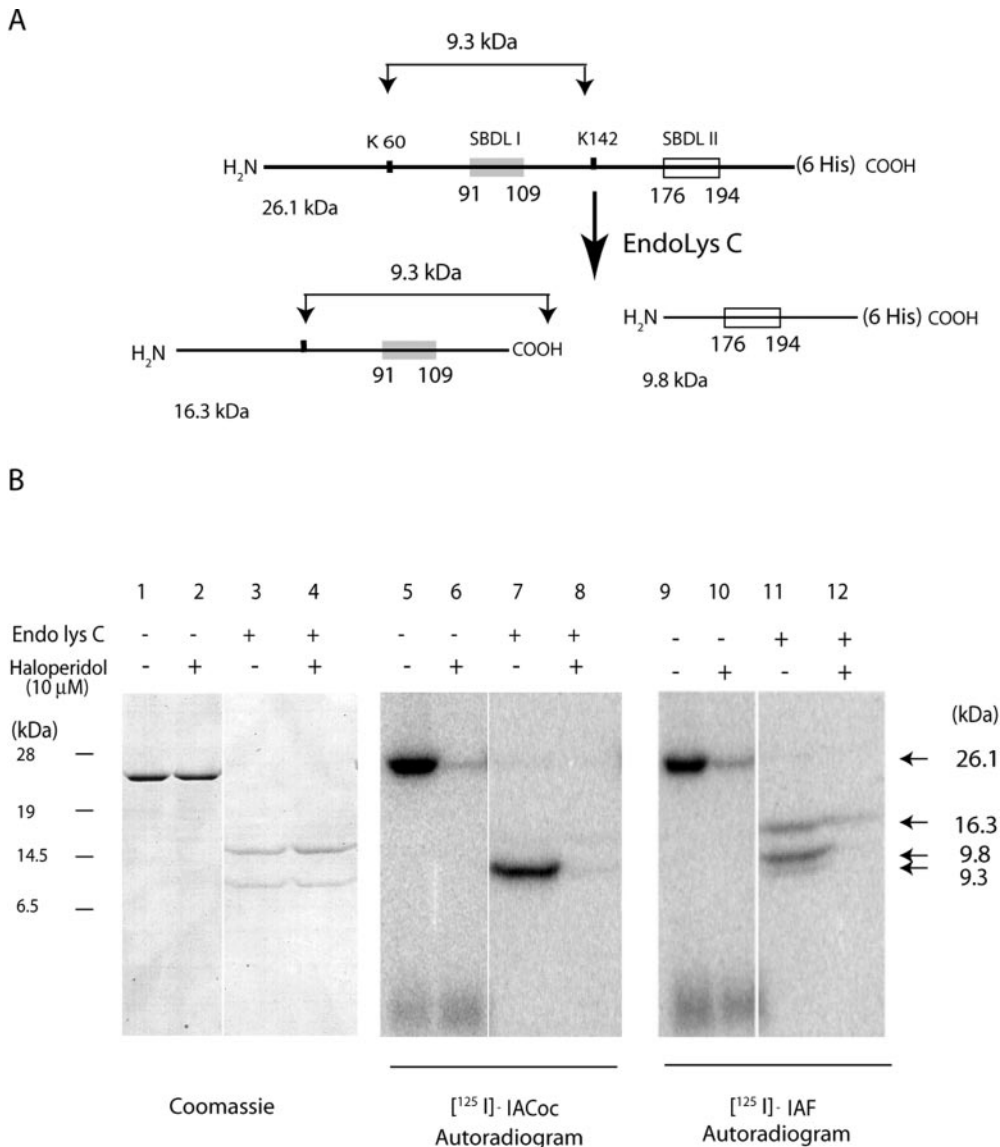


**Fig. 4.** A, schematic diagram of EndoLys-C cleavage of the pure six histidine tagged guinea pig  $\sigma$ -1 receptors. B, PhosphorImaging visualization of EndoLys-C cleavage of the pure guinea pig  $\sigma$ -1 receptor photolabeled with [ $^{125}$ I]IACoc and [ $^{125}$ I]IAF. Both [ $^{125}$ I]IACoc-photolabeled (lanes 5–8) and [ $^{125}$ I]IAF-photolabeled (lanes 9–12) pure guinea pig  $\sigma$ -1 receptor showed a similar EndoLys-C cleavage pattern as shown previously in Fig. 3C. In all cases, the specific labeling was determined by comparing the photolabeling of  $\sigma$ -1 receptor in the absence of 10  $\mu$ M haloperidol (lanes 5, 7, 9, and 11) and in the presence of 10  $\mu$ M haloperidol (lanes 6, 8, 10, and 12). Lanes 1 to 4 showed the Coomassie staining pattern of the [ $^{125}$ I]IACoc-photolabeled  $\sigma$ -1 receptors (lanes 5–8). The Coomassie staining for the [ $^{125}$ I]IAF-photolabeled  $\sigma$ -1 receptors was identical and is not shown here. Upon treatment with EndoLys-C, the specifically [ $^{125}$ I]IACoc-photolabeled receptors (lanes 5 and 6) resulted in two peptides with the molecular masses of 16.3 and 9.8 kDa. The specific radiolabel from [ $^{125}$ I]IACoc was located on the SBDLII region (9.8 kDa) (lanes 7 and 8). The specific [ $^{125}$ I]IAF-labeled  $\sigma$ -1 receptor (lanes 10–11), upon treatment with EndoLys-C, showed radiolabel on both the SBDLI (16.3 kDa) and SBDLII (9.8 kDa) regions (lanes 12 and 13). An additional specific radiolabeled band at 9.3 kDa (lane 12 and 13) was observed with [ $^{125}$ I]IAF consistent with the cleavage at the position 60 by EndoLys-C, which contains the SBDLI domain.

peptide containing the SBDLII domain (compare lanes 5 and 6 with 7 and 8, respectively, in Fig. 5B), which is again consistent with the pure guinea pig  $\sigma$ -1 receptor results (Fig. 4B) and data reported previously showing specific [ $^{125}$ I]IA-Coc photolabeling of COS7 cells transfected with guinea pig  $\sigma$ -1 receptor (Chen et al., 2007). Consistent with the results from membrane-bound  $\sigma$ -1 receptor, [ $^{125}$ I]IAF specifically labeled both the 16.3-kDa peptide containing SBDLI and the 9.8-kDa peptide containing SBDLII (compare lanes 9 and 10 with 11 and 12, respectively, in Fig. 5B). Specific label incorporation by [ $^{125}$ I]IAF was also observed again in the 9.3-kDa peptide consistent with partial EndoLys-C cleavage of the

pure guinea pig  $\sigma$ -1 receptor at position 60, which yielded a similar fragment containing SBDLI (lane 10, Fig. 5B).

As expected, cyanogen bromide cleavage of the [ $^{125}$ I]IA-Coc photolabeled 9.8-kDa fragment (Coomassie staining shown in lanes 2 and 4 in Fig. 5C) produced the specifically photolabeled 6.8-kDa fragment (compare lanes 6 and 8 in Fig. 5C), whereas no specific labeling of the CNBr-cleaved 16.3-kDa fragment (Coomassie staining shown in lanes 1 and 3 in Fig. 5C) by [ $^{125}$ I]IA-Coc was seen (compare lanes 5 and 7). CNBr cleavage of the [ $^{125}$ I]IAF-labeled 9.8-kDa band (Coomassie staining represented in lanes 2 and 4 in Fig. 5C) also produced the specifically labeled 6.8-kDa fragment (compare

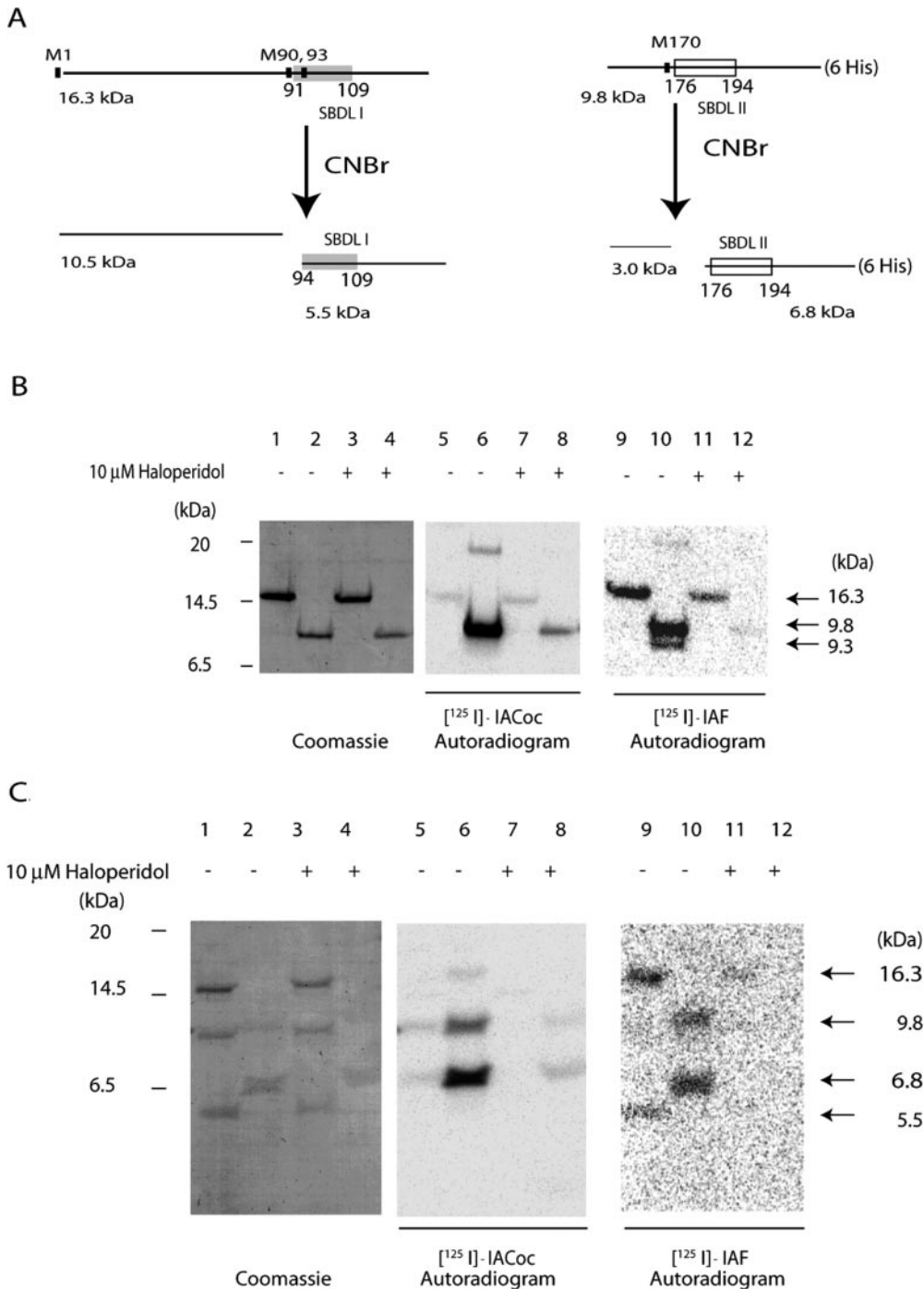


**Fig. 5.** A, schematic diagram of CNBr cleavage of the 16.3- and 9.8-kDa EndoLys-C cleaved peptides from pure guinea pig  $\sigma$ -1 receptors. B, gel-eluted EndoLys-C cleaved fragments of the pure guinea pig  $\sigma$ -1 receptor specifically photolabeled with [ $^{125}$ I]IA-Coc and [ $^{125}$ I]IAF. Because both [ $^{125}$ I]IA-Coc-photolabeled (lanes 5–8) and [ $^{125}$ I]IAF-photolabeled (lanes 9–12) EndoLys-C cleaved peptides showed similar Coomassie staining patterns, only the Coomassie staining pattern of the [ $^{125}$ I]IA-Coc-labeled peptides are shown (lanes 1–4). In all cases, the specific labeling was determined by comparing the photolabeling of  $\sigma$ -1 receptor in the absence of 10  $\mu$ M haloperidol (lanes 1 and 2, 5 and 6, and 9 and 10) and in the presence of 10  $\mu$ M haloperidol (lanes 3 and 4, 7 and 8, and 11 and 12). C, PhosphorImaging visualization of CNBr cleavage of the 16.3- and 9.8-kDa EndoLys-C cleaved peptides photolabeled with [ $^{125}$ I]IA-Coc and [ $^{125}$ I]IAF. Because both [ $^{125}$ I]IA-Coc- and [ $^{125}$ I]IAF-photolabeled CNBr cleaved peptides showed similar Coomassie staining patterns, only the Coomassie staining pattern for the [ $^{125}$ I]IA-Coc labeled peptides are shown (lanes 1–4). In all cases, the specific labeling was determined by comparing the photolabeling of the pure  $\sigma$ -1 receptor in the absence of 10  $\mu$ M haloperidol (lanes 1 and 2, 5 and 6, and 9 and 10) and in the presence of 10  $\mu$ M haloperidol (lanes 3 and 4, 7 and 8, and 11 and 12). Upon treatment with CNBr, the 16.3-kDa peptides (lanes 1 and 3) resulted in two peptides with molecular masses of 10.5 and 5.5 kDa (lanes 2 and 4), as depicted in Fig. 5A. The 10.5- and 5.5-kDa peptides were not specifically radiolabeled when [ $^{125}$ I]IA-Coc was used as the photoprobe (compare lanes 5 and 7). However, the same 16.3-kDa peptide that was specifically photolabeled with [ $^{125}$ I]IAF contained specific label in the SBDLI region (5.5-kDa fragments) (compare lane 9 with 11). Specific [ $^{125}$ I]IA-Coc and [ $^{125}$ I]IAF labeling that was found on the 9.8-kDa fragments upon treatment with CNBr was found on the 6.8-kDa fragments containing the SBDLII regions (compare lanes 6 and 10 with 8 and 12, respectively).

lanes 10 and 12 in Fig. 5C). On the other hand, CNBr cleavage of the [ $^{125}$ I]IAF-labeled 16.3-kDa fragment (Coomassie staining depicted in lanes 1 and 3 in Fig. 5C) produced the specifically labeled 5.5-kDa fragment (compare lanes 9 and 11 in Fig. 5C) containing the SBDLI domain. All of these results together support the conclusion that the [ $^{125}$ I]IAF photoprobe inserts into peptides containing the sequences identified as the SBDLI (amino acids 91–109) and SBDLII (amino acids 176–194).

## Discussion

Fenpropimorph, a yeast sterol isomerase inhibitor, has been found previously to bind with high affinity to the guinea pig  $\sigma$ -1 receptor ( $K_i = 0.005$  nM) (Moebius et al., 1997). This is perhaps not surprising, because the  $\sigma$ -1 receptor shows sequence homology with the C8–C7 yeast sterol isomerase (Moebius et al., 1996; Jbilo et al., 1997; Moebius et al., 1997). In an effort to find specific, high-affinity ligands and photoprobes for the  $\sigma$ -1 and  $\sigma$ -2 receptors, we have synthesized various derivatives of fenpropimorph as outlined in Schemes 1 and 2. The affinities of these fenpropimorph derivatives were determined by competition with (+)-[ $^3$ H]pentazocine for binding to the  $\sigma$ -1 receptor. The affinity of IAF (compound **10**) for the  $\sigma$ -2 receptor was determined by competitive binding of [ $^3$ H]DTG in the presence of nonradioactive (+)-pentazocine. Compound **2** was found not to bind to the  $\sigma$ -1 receptor ( $K_D > 100$   $\mu$ M), presumably because its amide group traps the nitrogen's lone pair needed for optimal binding (Ablordeppey et al., 2000). Compounds **3** and **11**, on the other hand, had the highest binding affinities to the  $\sigma$ -1 receptor with  $K_D$  values of less than 100 nM. IAF (compound **10**) bound with nearly 14.3-fold higher affinity to the  $\sigma$ -1 receptor ( $K_D = 194 \pm 27.5$  nM) over the  $\sigma$ -2 receptor ( $K_D = 2.78 \pm 1.5$   $\mu$ M) and was derivatized as a radioiodinated photoaffinity label. Figure 1, A and B, show that [ $^{125}$ I]IAF does indeed photolabel the  $\sigma$ -1 and  $\sigma$ -2 receptors in a specific and protectable manner. The  $\sigma$ -1 receptor at 25.3 kDa is protected by nonradioactive (+)-pentazocine, DTG, haloperidol, and fenpropimorph, whereas the  $\sigma$ -2 receptor at 18 kDa is protected by all of the compounds listed except for the  $\sigma$ -1-specific ligand (+)-pentazocine. Figure 1A illustrates that the photoaffinity label previously synthesized in our laboratory, [ $^{125}$ I]IACoc (Kahoun and Ruoho, 1992), derivatized the  $\sigma$ -1 receptor specifically. It is interesting that, as shown in Fig. 2, A and B, high molecular mass bands are present, which were derivatized by both radioiodinated photoaffinity labels and were protected by (+)-pentazocine, haloperidol, DTG, and fenpropimorph. The molecular masses of these protein bands were identified as 96.7, 130, and 147 kDa, with ligand binding properties consistent with the  $\sigma$ -1 receptor. It is significant the  $\sigma$ -1 receptor contains two GXXXG motifs, which occur with high frequency in membrane proteins that favor helix-helix interactions (Brosig and Langosch, 1998; Russ and Engelman, 2000; Kleiger et al., 2002; Polgar et al., 2004). Further investigation is required to characterize these high molecular mass bands and determine whether they are homo- or heterooligomers of the  $\sigma$ -1 receptor or whether they interact with other membrane proteins.

In addition to the highly specific labeling of the  $\sigma$ -1 (25.3 kDa) and  $\sigma$ -2 (18 kDa) receptors in rat liver membranes (Fig. 2, A and B), it was observed that a 19-kDa protein was also

labeled, which was protectable by fenpropimorph but not by other traditional  $\sigma$  ligands. The appearance of the selective [ $^{125}$ I]IAF labeling of this 19-kDa band raises the possibility that this band may represent the emopamil binding protein-like protein previously identified by Moebius et al. (2003).

The position of [ $^{125}$ I]IACoc binding of the guinea pig  $\sigma$ -1 receptor has been identified previously in the third hydrophobic region of the  $\sigma$ -1 receptor, which has high sequence homology to the yeast and fungal sterol isomerase (Chen et al., 2007). The specific amino acid that was identified as a photo-insertion site with [ $^{125}$ I]IACoc was Asp188. We have designated this region as SBDLII (amino acids 176–194) (Chen et al., 2007). From similar sequence homology considerations, a second region of the guinea pig and rat  $\sigma$ -1 receptor (amino acids 91–109), which matches the sequence of the yeast sterol isomerase, has been designated as SBDLI (Chen et al., 2007).

The specific [ $^{125}$ I]IACoc and [ $^{125}$ I]IAF photolabeled  $\sigma$ -1 receptors in the natural milieu of the membranes (i.e., in guinea pig and rat liver membranes) resulted in two identical peptides having molecular masses of 16.3 and 9 kDa after cleavage with the protease EndoLys-C (Fig. 3C). The haloperidol protectable label incorporation for both [ $^{125}$ I]IACoc and [ $^{125}$ I]IAF was in the SBDLII containing peptide (9 kDa). In addition, the haloperidol-protectable photolabeling was also found in the 16.3 kDa fragment that contains SBDLI with [ $^{125}$ I]IAF used as the photoprobe (Fig. 3C). The amount of specific [ $^{125}$ I]IAF labeling between the 9- and 16.3-kDa fragments seemed to differ between the rat liver membrane  $\sigma$ -1 receptor and guinea pig liver membrane  $\sigma$ -1 receptor (compare lanes 7, 8, 15, and 16 in Fig. 3C), which perhaps could be caused by subtle differences in the binding site of the  $\sigma$ -1 receptor in the membrane preparations from the two species. An additional observation in the EndoLys-C cleavage experiments that was repeatedly observed was that the guinea pig  $\sigma$ -1 receptor, which contains a lysine at position 60, was not cleaved by the enzyme as would be predicted. The reason for the lack of cleavage by EndoLys-C in guinea pig  $\sigma$ -1 receptor at position 60 is not readily explained but may be caused by a conformational constraint or otherwise lack of access for the proteolytic enzyme. On the other hand, the rat  $\sigma$ -1 receptor contains an arginine at position 60 and is, therefore, not expected to be cleaved by EndoLys-C.

The pure guinea pig  $\sigma$ -1 receptor, photolabeled with both [ $^{125}$ I]IACoc and [ $^{125}$ I]IAF, also showed similar EndoLys-C cleavage patterns (Fig. 4B) compared with guinea pig and rat liver membranes (shown in Fig. 3C). The specific [ $^{125}$ I]IACoc labeling was found only on the 9.8-kDa peptide that contains the SBDLII (Fig. 4B, lanes 7 and 8), and the specific [ $^{125}$ I]IAF labeling was found on both the 16.3- and 9.8-kDa peptides (Fig. 4B, lanes 11 and 12). When further cleaved with cyanogen bromide, the [ $^{125}$ I]IAF-labeled 16.3 and 9.8-kDa peptides resulted in peptides of molecular masses of 5.5 kDa (amino acids 94–142) and 6.8 kDa (amino acids 171–229) that contained the SBDLI and the SBDLII domains, respectively, and were radiolabeled (Fig. 5C, lanes 9 and 10) as described in Fig. 5A. Both the competitive binding data (Fig. 1 and Table 1) for IAF versus (+)-[ $^3$ H]pentazocine and the IAF photoprobe data indicate a single binding site or two binding sites with equal affinity. Together, these observations suggest that the  $\sigma$ -1 receptor contains a haloperidol-protectable ligand binding site(s) for IAF that is composed, at least in part, of

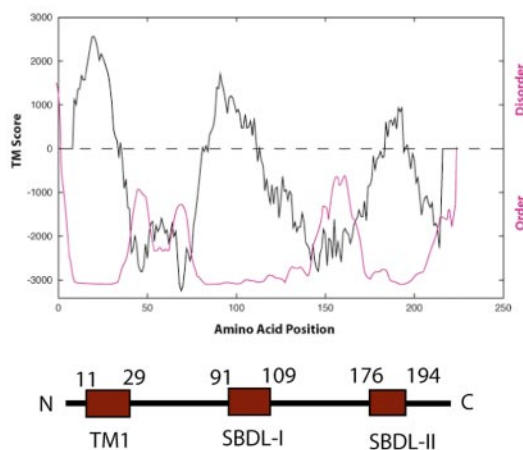
the SBDLI and SBDLII domains. The photoreactive azido group in [<sup>125</sup>I]IAF may interact with both the SBDLI and SBDLII domains because of the flexibility of the molecule. [<sup>125</sup>I]IACoc, on the other hand, interacts only with the SBDLII region because of the structural rigidity and restricted motion of the tropane ring.

As reported previously (Aydar et al., 2002), the  $\sigma$ -1 receptor contains an even number of transmembrane sequences because both the N and C termini lie on the same side of a biological membrane. Hydrophobicity analysis of the  $\sigma$ -1 receptor (using the prediction program available at [http://www.ch.embnet.org/software/TMPRED\\_form.html](http://www.ch.embnet.org/software/TMPRED_form.html)) identifies three hydrophobic regions as illustrated in Fig. 6A. The alignment of the  $\sigma$ -1 receptor sequence reasonably aligns the first hydrophobic region with transmembrane domain I (TMD I) and the second hydrophobic sequence with TMD II. From sequence alignment, the sequence of the amino acids 90 to 110 of the  $\sigma$ -1 receptor matched with high fidelity to the yeast and fungal sterol isomerase (Hanner et al., 1996; Chen et al., 2007). This region partially overlaps putative TMD II and constitutes SBDLI (amino acids 91–109). The third hydrophobic region, which aligns with the SBDLII region, is the location of Asp188, which is specifically photolabeled by [<sup>125</sup>I]IACoc (Chen et al., 2007). Additional support for this positioning of TMD segments is consistent with a PONDR

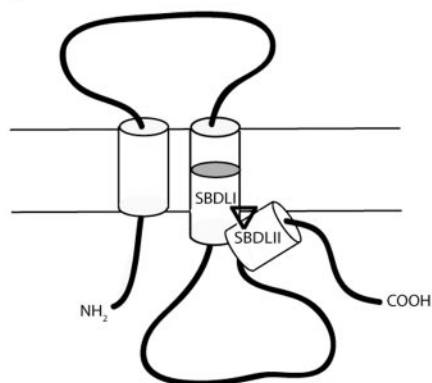
program (available at <http://www.pondr.com/background.html>) acquisition of the  $\sigma$ -1 receptor that evaluates relative order versus disorder profiles of a protein. Using this analysis (Fig. 6A), the hydrophobic regions proposed as TMDI and TMDII and the SBDLI and SBDLII regions are highly ordered and possibly feature an  $\alpha$ -helical structure. Therefore, in Fig. 6, B and C, the hydrophobic regions are diagrammed as cylinders to depict  $\alpha$  helices.

In summary, we report the synthesis of various fenpropion derivatives and their binding affinities as ligands for the  $\sigma$ -1 receptor. We have also demonstrated that the radioiodinated photoaffinity label [<sup>125</sup>I]IAF is able to specifically photolabel  $\sigma$ -1 and  $\sigma$ -2 receptors. Photolabeling with [<sup>125</sup>I]IAF and [<sup>125</sup>I]IACoc further identified high molecular mass protein complexes that were not completely dissociated upon SDS-PAGE analysis. The data suggest that  $\sigma$ -1 receptors may exist as oligomers or interact with protein partners either constitutively or through binding of ligands. Based on the simultaneous specific photolabeling of SBDLI- and SBDLII-containing peptides in the guinea pig  $\sigma$ -1 receptor by [<sup>125</sup>I]IAF and the fact that there is haloperidol-protectable binding of IAF to the  $\sigma$ -1 receptor, the data reported in this article support the conclusion that SBDLI and SBDLII comprise at least portions of the  $\sigma$ -1 receptor ligand binding

A



B



C

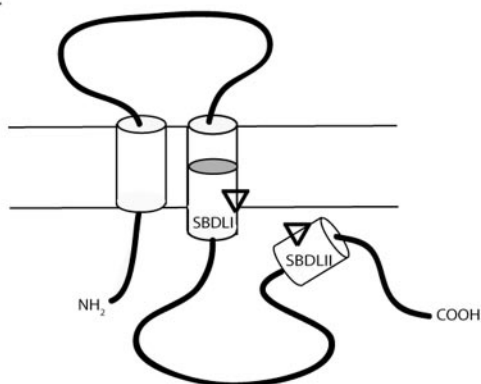


**Fig. 6.** A, SBDLI and SBDLII regions of the  $\sigma$ -1 receptor. Hydrophobic regions of the protein, which are predicted by the TMPred program (available at [http://www.ch.embnet.org/software/TMPRED\\_form.html](http://www.ch.embnet.org/software/TMPRED_form.html)) and the PONDR program (available at <http://www.pondr.com/background.html>), were used to predict the transmembrane segments and areas of order and disorder. Three highly ordered hydrophobic regions are shown, the latter two of which contain the highly conserved SBDLI and SBDLII regions, respectively. B, a putative model of the  $\sigma$ -1 receptor illustrates a possible spatial arrangement of the ligand binding site in which the cylinders depict the hydrophobic regions as putative  $\alpha$  helices and [<sup>125</sup>I]IAF as  $\nabla$ . C, an alternative model for IAF interaction with the  $\sigma$ -1 receptor is depicted in B.

site(s) and suggest possible folded structures as portrayed in Fig. 6, B and C.

#### Acknowledgments

We acknowledge insights and assistance from Dr. Michael K. Sievert and from Dr. Anupama Gopalakrishnan for proofreading of the manuscript.

#### References

- Ablordepey SY, Fischer JB, and Glennon RA (2000) Is a nitrogen atom an important pharmacophoric element in sigma ligand binding? *Bioorg Med Chem* **8**:2105–2111.
- Aydar E, Palmer CP, Klyachko VA, and Jackson MB (2002) The sigma receptor as a ligand-regulated auxiliary potassium channel subunit. *Neuron* **34**:399–410.
- Brosig B and Langosch D (1998) The dimerization motif of the glycoprotein A transmembrane segment in membranes: importance of glycine residues. *Protein Sci* **7**:1052–1056.
- Chen Y, Hajipour AR, Sievert MK, Arbabian M, and Ruoho AE (2007) Characterization of the cocaine binding site on the sigma-1 receptor. *Biochemistry* **46**:3532–3542.
- Cheng Y and Prusoff WH (1973) Relationship between the inhibition constant (K<sub>1</sub>) and the concentration of inhibitor which causes 50 per cent inhibition (I<sub>50</sub>) of an enzymatic reaction. *Biochem Pharmacol* **22**:3099–3108.
- Hajipour AR, Adibi H, and Ruoho AE (2003) Wet silica-supported permanganate for the cleavage of semicarbazones and phenylhydrazones under solvent-free conditions. *J Org Chem* **68**:4553–4555.
- Hajipour AR, Kooshki B, and Ruoho AE (2005a) Nitric acid and phosphorus pentoxide supported on silica gel as a mild and efficient system for the oxidation of benzylic alcohols under solvent-free conditions. *Org Prep Proced Int* **37**:585–589.
- Hajipour AR, Kooshki B, and Ruoho AE (2005b) Nitric acid in the presence of supported P<sub>2</sub>O<sub>5</sub> on silica gel: an efficient and novel reagent for oxidation of sulfides to the corresponding sulfoxides. *Tetrahedron Lett* **46**:5503–5506.
- Hajipour AR and Ruoho AE (2005a) Methyltriphenylphosphonium peroxydisulfate and iodine as mild reagents for the iodination of activated aromatic compounds. *Org Prep Proced Int* **37**:279–283.
- Hajipour AR and Ruoho AE (2005b) Nitric acid in the presence of P<sub>2</sub>O<sub>5</sub> supported on silica gel—a useful reagent for nitration of aromatic compounds under solvent-free conditions. *Tetrahedron Lett* **46**:8307–8310.
- Hanner M, Moebius FF, Flandorfer A, Knaus HG, Striessnig J, Kempner E, and Glossmann H (1996) Purification, molecular cloning, and expression of the mammalian  $\sigma$ 1-binding site. *Proc Natl Acad Sci U S A* **93**:8072–8077.
- Hayashi T and Su TP (2001) Regulating ankyrin dynamics: Roles of  $\sigma$ -1 receptors. *Proc Natl Acad Sci U S A* **98**:491–496.
- Hayashi T and Su TP (2003)  $\sigma$ -1 Receptors ( $\sigma$ <sub>1</sub> binding sites) form raft-like microdomains and target lipid droplets on the endoplasmic reticulum: roles in endoplasmic reticulum lipid compartmentalization and export. *J Pharmacol Exp Ther* **306**:718–725.
- Iwamoto ET (1981) Locomotor activity and antinociception after putative mu, kappa and  $\sigma$  opioid receptor agonists in the rat: influence of dopaminergic agonists and antagonists. *J Pharmacol Exp Ther* **217**:451–460.
- Jbilo O, Vidal H, Paul R, De Nys N, Bensaid M, Silve S, Carayon P, Davi D, Galiegue S, Bourrie B, et al. (1997) Purification and characterization of the human SR 31747A-binding protein. A nuclear membrane protein related to yeast sterol isomerase. *J Biol Chem* **272**:27107–27115.
- Kahoun JR and Ruoho AE (1992) [<sup>125</sup>I]Iodoazidococaine, a photoaffinity label for the haloperidol-sensitive  $\sigma$  receptor. *Proc Natl Acad Sci U S A* **89**:1393–1397.
- Kekuda R, Prasad PD, Fei YJ, Leibach FH, and Ganapathy V (1996) Cloning and functional expression of the human type 1 sigma receptor (hSigmaR1). *Biochem Biophys Res Commun* **229**:553–558.
- Kleiger A, Grothe R, Mallick P, and Eisenberg D (2002) GXXXG and AXXXA: common alpha-helical interaction motifs in proteins, particularly in extremophiles. *Biochemistry* **41**:5990–5997.
- Langa F, Codony X, Tovar V, Lavado A, Gimenez E, Cozar P, Cantero M, Dordal A, Hernandez E, Perez R, et al. (2003) Generation and phenotypic analysis of sigma receptor type I (sigma 1) knockout mice. *Eur J Neurosci* **18**:2188–2196.
- Lysko PG, Gagnon RC, Yue TL, Gu JL, and Feuerstein G (1992) Neuroprotective effects of SKF 10,047 in cultured rat cerebellar neurons and in gerbil global brain ischemia. *Stroke* **23**:414–419.
- Martin WR, Eades CG, Thompson JA, Huppler RE, and Gilbert PE (1976) The effects of morphine- and nalorphine-like drugs in the nondependent and morphine-dependent chronic spinal dog. *J Pharmacol Exp Ther* **197**:517–532.
- Matsumoto RR, Bowen WD, Tom MA, Vo VN, Truong DD, and De Costa BR (1995) Characterization of two novel sigma receptor ligands: antidystonic effects in rats suggest sigma receptor antagonism. *Eur J Pharmacol* **280**:301–310.
- Matsuno K, Matsunaga K, Senda T, and Mita S (1993) Increase in extracellular acetylcholine level by  $\sigma$  ligands in rat frontal cortex. *J Pharmacol Exp Ther* **265**:851–859.
- McCracken KA, Bowen WD, de Costa BR, and Matsumoto RR (1999a) Two novel sigma receptor ligands, BD1047 and LR172, attenuate cocaine-induced toxicity and locomotor activity. *Eur J Pharmacol* **370**:225–232.
- McCracken KA, Bowen WD, and Matsumoto RR (1999b) Novel sigma receptor ligands attenuate the locomotor stimulatory effects of cocaine. *Eur J Pharmacol* **365**:35–38.
- Mei J and Pasternak GW (2001) Molecular cloning and pharmacological characterization of the rat sigma1 receptor. *Biochem Pharmacol* **62**:349–355.
- Moebius FF, Bermoser K, Reiter RJ, Hanner M, and Glossmann H (1996) Yeast sterol C8–C7 isomerase: identification and characterization of a high-affinity binding site for enzyme inhibitors. *Biochemistry* **35**:16871–16878.
- Moebius FF, Fitzky BU, Wietzorrek G, Haidekker A, Eder A, and Glossmann H (2003) Cloning of an emopamil-binding protein (EBP)-like protein that lacks sterol delta8-delta7 isomerase activity. *Biochem J* **374**:229–237.
- Moebius FF, Reiter RJ, Hanner M, and Glossmann H (1997) High affinity of sigma 1-binding sites for sterol isomerization inhibitors: evidence for a pharmacological relationship with the yeast sterol C8–C7 isomerase. *Br J Pharmacol* **121**:1–6.
- Nguyen EC, McCracken KA, Liu Y, Pouw B, and Matsumoto RR (2005) Involvement of sigma (sigma) receptors in the acute actions of methamphetamine: receptor binding and behavioral studies. *Neuropharmacology* **49**:638–645.
- Pan YX, Mei J, Xu J, Wan BL, Zuckerman A, and Pasternak GW (1998) Cloning and characterization of a mouse sigma1 receptor. *J Neurochem* **70**:2279–2285.
- Paul R, Lavastre S, Floutard D, Floutard R, Canat X, Casellas P, Le Fur G, and Breliere JC (1994) Allosteric modulation of peripheral sigma binding sites by a new selective ligand: SR 31747. *J Neuroimmunol* **52**:183–192.
- Polgar O, Robey RW, Morisaki K, Dean M, Michejda C, Sauna ZE, Ambudkar SV, Tarasova N, and Bates SE (2004) Mutational analysis of ABCG2: role of the GXXXG motif. *Biochemistry* **43**:9448–9456.
- Prasad PD, Li HW, Fei YJ, Ganapathy ME, Fujita T, Plumley LH, Yang-Feng TL, Leibach FH, and Ganapathy V (1998) Exon-intron structure, analysis of promoter region, and chromosomal localization of the human type 1 sigma receptor gene. *J Neurochem* **70**:443–451.
- Quirion R, Bowen WD, Itzhak Y, Junien JL, Musacchio JM, Rothman RB, Su TP, Tam SW, and Taylor DP (1992) A proposal for the classification of sigma binding sites. *Trends Pharmacol Sci* **13**:85–86.
- Ramachandran S, Lu H, Prabhu U, and Ruoho AE (2007) Purification and characterization of the guinea pig sigma-1 receptor functionally expressed in *Escherichia coli*. *Protein Expr Purif* **51**:283–292.
- Russ WP and Engelman DM (2000) The GxxxG motif: a framework for transmembrane helix-helix association. *J Mol Biol* **296**:911–919.
- Seth P, Fei YJ, Li HW, Huang W, Leibach FH, and Ganapathy V (1998) Cloning and functional characterization of a sigma receptor from rat brain. *J Neurochem* **70**:922–931.
- Su TP (1982) Evidence for  $\sigma$  opioid receptor: binding of [<sup>3</sup>H]SKF-10047 to etorphine-inaccessible sites in guinea-pig brain. *J Pharmacol Exp Ther* **223**:284–290.
- Vaupel DB (1983) Naltrexone fails to antagonize the sigma effects of PCP and SKF 10,047 in the dog. *Eur J Pharmacol* **92**:269–274.
- Wilke RA, Mehta RP, Lupardus PJ, Chen Y, Ruoho AE, and Jackson MB (1999)  $\sigma$  Receptor photolabeling and  $\sigma$  receptor-mediated modulation of potassium channels in tumor cells. *J Biol Chem* **274**:18387–18392.

**Address correspondence to:** Dr. Arnold E. Ruoho, Department of Pharmacology, University of Wisconsin Medical School, 1300 University Avenue, Madison, WI 53706. E-mail: aeruoho@wisc.edu